Materials Science & Engineering A 716 (2018) 228–234

Contents lists available at ScienceDirect

Materials Science & Engineering A

journal homepage: www.elsevier.com/locate/msea

Fractographic analysis of fatigue crack initiation and propagation in CP titanium with a bimodal harmonic structure

Yuhei Nukui[a], Hiroki kubozono[a], Shoichi kikuchi[a,*], Yoshikazu nakai[a], Akira ueno[b], Mie Ota kawabata[b], Kei ameyama[b]

[a] Department of Mechanical Engineering, Graduate School of Engineering, Kobe University, 1-1 Rokkodai-cho, Nada-ku, Kobe 657-8501, Japan
[b] Department of Mechanical Engineering, College of Science and Engineering, Ritsumeikan University, 1-1-1 Noji-higashi, Kusatsu, Shiga 525-8577, Japan

ARTICLE INFO

Keywords:
Fatigue
Fracture mechanics
Titanium
Fractography
Grain refinement
EBSD

ABSTRACT

Commercially pure (CP) titanium with a bimodal harmonic structure, which is defined as coarse grained regions surrounded by a network of fine grains, was fabricated by consolidating mechanically milled powders to improve both strength and ductility. In order to determine the fatigue properties of bimodal harmonic structured CP titanium, four-point bending fatigue tests were conducted at a stress ratio of 0.1 under ambient conditions. The fracture surfaces were analyzed by scanning electron microscopy (SEM) and electron backscatter diffraction (EBSD) to identify the mechanisms of small fatigue crack initiation and propagation on the basis of fractography and crystallography. The fatigue crack initiation resistance was increased compared to sintered compacts fabricated from as-received initial powders, which was attributed to grain refinement during mechanical milling. Transgranular fracture occurred from coarse grains with a basal plane perpendicular to the loading direction. The fatigue crack path in harmonic structured CP titanium was not influenced by the microstructure.

1. Introduction

Commercially pure (CP) titanium has been used in various engineering fields and products, such as civilian goods and biomaterials for the replacement of bone tissue, because it exhibits high corrosion resistance and good biocompatibility [1]. Recent years have seen an increase in the demand for CP titanium with improved mechanical properties. Thus, increasing the structural reliability of CP titanium has become an important research area. Grain refinement through severe plastic deformation is generally an effective approach for strengthening metallic materials such as light alloys [2], titanium alloys [3], and CP titanium [4–10], on the basis of the Hall-Petch relationship [11,12].

In the case of CP titanium, however, in order to prevent a decrease in ductility due to a homogeneous fine-grained structure [6,9,10], various bimodal microstructural designs have been proposed [13–17]. Our group has developed a harmonic structure using powder metallurgy to consolidate mechanically milled CP titanium powders [18–21], which improves both their strength and ductility by suppressing necking during tensile deformation [22]. In particular, we have focused on the fatigue properties [23–25] and the near-threshold propagation of long fatigue cracks [26–28], which depend on the stress ratio (the ratio of the minimum to maximum stress), for CP titanium and Ti-6Al-4V with a bimodal harmonic structure. It was found that the harmonic structure increases the fatigue limit for Ti-6Al-4V [23–25], but decreases the resistance to long crack propagation in both CP titanium [26] and Ti-6Al-4V [27,28]. It is also important to investigate the propagation of small fatigue cracks in the newly developed CP titanium, since there are differences in the threshold stress intensity range, ΔK_{th}, for small and long fatigue cracks [29,30]. Thus, both the initiation and propagation of small fatigue cracks must be examined in bimodal harmonic structured CP titanium in order to achieve sufficient performance in newly designed materials for practical applications.

Fractography and microstructural observations are effective for identifying fracture mechanisms. Ueno et al. [31] examined the fracture mechanism in bimodal harmonic structured stainless steel under tension through detailed stereographic observations, and confirmed that cracks propagated along the interface between the coarse and fine grained regions. Szczepanski et al. [32] conducted orientation imaging microscopy (OIM) scans at fatigue crack initiation sites and measured the spatial orientations of facets using stereography. Their results indicated that fatigue cracks in Ti-6Al-2Sn-4Zr-6Mo were initiated at facets formed by the fracture of the large primary α grains preferentially oriented to allow either basal or prismatic slip. Uematsu et al. [33] conducted a fractographic analysis of fatigue crack initiation using electron backscatter diffraction (EBSD) on the cross section of a Ti-22V-4Al alloy specimen and found that glide-plane decohesion or cleavage

* Corresponding author.
E-mail address: kikuchi@mech.kobe-u.ac.jp (S. kikuchi).

https://doi.org/10.1016/j.msea.2018.01.054
Received 24 November 2017; Received in revised form 11 January 2018; Accepted 12 January 2018
Available online 30 January 2018
0921-5093/

of the α phase was responsible for crack initiation in the material. The authors [24] have developed a method for characterizing the crystal orientation of the facets observed on fracture surfaces through a combination of EBSD and fracture surface analysis to identify the fatigue fracture mechanism in Ti-6Al-4V with a bimodal harmonic structure.

The purpose of the present study is to examine fatigue crack initiation in bimodal harmonic structured CP titanium under four-point bending on the basis of fractography and crystallography. Furthermore, the effects of the bimodal harmonic structure on small fatigue crack propagation in CP titanium are examined.

2. Experimental

2.1. Materials

This study utilized CP titanium containing 0.01% C, 0.10% O, 0.004% N, and 0.02% Fe (all by mass, with the balance being Ti). The material was made into a powder (126-μm particle diameter) by a plasma rotating electrode process that can be used to fabricate spherical particles with negligible amounts of contaminants like oxygen and nitrogen gas [34].

Bimodal microstructural design through mechanical milling (MM) and spark plasma sintering (SPS) was employed to form “harmonic structured” CP titanium, as defined below. MM of the CP titanium powders was performed for 360 ks in an Ar atmosphere at room temperature using a planetary ball mill (Fritch P-5) with a tungsten carbide vessel and steel ball bearings to form fine grains at the particle surfaces. The rotation speed was set to 200 rpm, and the ball-to-powder mass ratio was 1.8:1. The powders were then consolidated by SPS at 1073 K for 600 s in a vacuum (around 10 Pa) and under applied pressure (50 MPa) using a 25-mm internal diameter graphite die to produce the specimens referred to herein as the “MM series.” For comparison, a second set of specimens was prepared by sintering the as-received powders (hereafter, “untreated series”). The tensile strength of the MM series (620 MPa) was higher than that of the untreated series (490 MPa), yet the MM series exhibited almost the same elongation as the untreated series in a previous study [35].

The microstructure of sintered compacts was characterized after chemical etching with Kroll's solution. A scanning electron microscopy (SEM) image of a sample produced by MM is shown in Fig. 1. The microstructure consists of a mixture of coarse grained regions surrounded by fine equiaxed grains to form a continuous three-dimensional network. This is referred to as a “harmonic” structure throughout this paper. A previous study found that the area fraction of the fine grains was as high as 31% for the MM series, where “fine” is defined as smaller than 10 μm [26]. Furthermore, the average size of the coarse grains (25.9 μm) was smaller than the average grain size in the untreated series (122 μm).

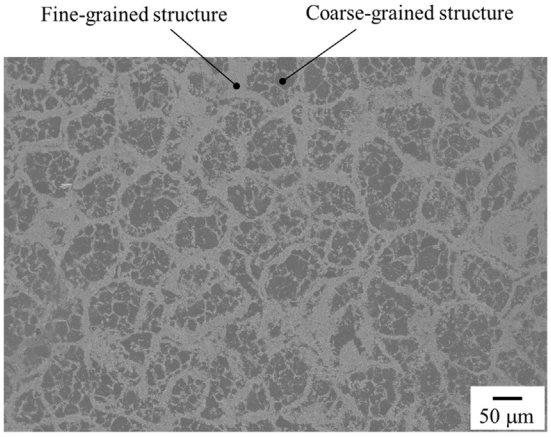

Fig. 1. SEM micrograph of MM series etched with Kroll's solution.

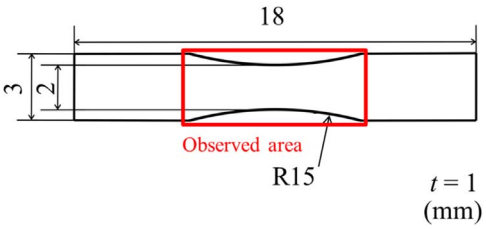

Fig. 2. Specimen dimensions.

2.2. Fatigue tests

The sintered material (10 mm thick, 25 mm diameter) was sliced into ~ 1.5-mm-thick disks, each of which was machined into a blunt-notched specimen with the dimensions shown in Fig. 2. The specimen surface was then polished using emery paper (#240 to #4000) to a thickness of 1 mm and polished further in a SiO_2 suspension to obtain a mirror finish. In order to remove the electro-discharge machined layer, the notch roots of the specimens were also polished with emery paper (#240).

An electrodynamic fatigue testing system was used to perform four-point bending tests under a stress ratio R of 0.1. The stress cycling frequency was 10 Hz, and the tests were conducted under ambient conditions. Fatigue tests were interrupted after a certain number of cycles and acetyl cellulose films were placed on the specimen surface (“Observed area” in Fig. 2) using the replica method to examine fatigue crack initiation and propagation. Once the crack length was measured using optical microscopy, the stress intensity range, ΔK, was calculated [36]; the aspect ratio, c/a, for small cracks was estimated using

$$c/a = 1 - 1.607(a/t) + 1.080(a/t)^2 - 0.2149(a/t)^3 \quad \text{for } a/t < 1 \text{ and} \tag{1}$$

$$c/a = 0.259 \quad \text{for } a/t \geq 1, \tag{2}$$

where a is the crack length on the surface, c is the crack length along the thickness direction, and t is the specimen thickness.

After the fatigue tests, fracture surfaces and the fatigue crack paths were observed by SEM to determine the mechanism for small fatigue crack initiation and propagation. Furthermore, the microstructure near the crack initiation site was observed by EBSD at an acceleration voltage of 20 kV.

3. Results and discussion

3.1. S-N characteristics of harmonic structured CP titanium

The results of four-point bending fatigue tests for the sintered compacts (untreated and MM series) are shown in Fig. 3 in terms of the stress amplitude, σ_a, applied to the specimen surface as a function of the number of cycles to failure, N_f. The data points indicated by arrows represent the run-out specimens that have failure at $N = 10^7$ cycles.

The fact that both the MM series and the untreated series failed at $\sigma_a = 160$ MPa but not at $\sigma_a = 150$ MPa indicates that their fatigue limits, σ_w, were comparable. In addition, at $\sigma_a = 200$ MPa, the fatigue lives of the specimens in the MM series exhibited a large scatter, with some not undergoing failure at all. This can be attributed to the unique microstructure of the MM series, and suggests that their fatigue properties are somewhat better than those of the untreated series.

The fracture surfaces were observed by SEM to determine the fatigue properties for both series in more detail. Fig. 4 shows SEM fractographs of specimens of the untreated series ($N_f = 3.27 \times 10^5$ cycles) and MM series ($N_f = 4.91 \times 10^6$ cycles) that failed at $\sigma_a = 160$ MPa. Fracture surface 1 is shown in a mirror-reversed image in both series to